Three-Dimensional Aeroelastic Computation Based on Stationary Body-Conforming Grids with Small Perturbation Boundary Conditions

Shuchi Yang*, Feng Liu†, Shijun Luo‡
Department of Mechanical and Aerospace Engineering
University of California, Irvine, CA 92697-3975

Her-Mann Tsai§
Temasek Laboratories
National University of Singapore
Kent Ridge Crescent, Singapore 119260

David M. Schuster¶
Aeroelasticity Branch
NASA Langley Research Center, Hampton, VA 23681

The authors developed an approximate-boundary-condition method for time-domain aeroelastic simulations on stationary body-conforming grids (AIAA 2004-0885). This method is extended to three dimensions in this paper. The CFD solver with the approximate boundary conditions is coupled with elastic equations to predict the aeroelastic properties of wings. The accurate nonlinear Euler equations are solved in the field, while the movement of the solid surfaces is accounted for in the approximate boundary conditions without moving or deforming the computational grids. The first-order approximate wall-boundary conditions are used in solving the full Euler equations. Results are compared with Euler solutions with the full boundary conditions on moving grids and known experimental data.

I Introduction

In recent years, high level computational fluid dynamics methods are successfully used to predict flutter for complex configurations.[1] However, development of efficient and robust schemes for grid deformation is still a challenge and difficulty for computational aeroelastic (CAE), especially for time-domain simulation using Euler or Reynolds-Averaged Navier-Stokes(RANS) equations(see Ref. 1 for a review). For most Euler or RANS solvers used in CAE, the full surface boundary condition is implemented and the physical motion of the boundary is captured directly in equation of motion. This kind of treatment is accurate but it introduces a major complication to the analysis. Efficiently moving millions of computation grid points thousands of times in an aeroelastic computation process have to be accomplished. Furthermore, degradation of grid quality and grid crossing may decrease computation accuracy or terminate the computation. In this aspect, the TSD(Transonic Small Disturbance) method eliminates the physical deformation by assuming small perturbation. For TSD potential method, for example,the NASA Langley CAP-TSD code,[2–4] the movement of the wall surface is accounted for in the boundary condition so that the computational grid is always stationary. In an effort to take advantage of a stationary grid while eliminating the limitations of the small-perturbation potential model, Gao, Luo, Liu, and Schuster[5, 6] presented an unsteady Euler method using stationary Cartesian grid for thin airfoils. Recently Yang, Liu, Luo, and Schuster[7] implemented this concept on stationary body-conforming curvilinear grids in order to improve the Cartesian grid method, especially to remove the limitation of thin airfoil assumption and the singularity for blunt leading edge which occurs on Cartesian grid.[5, 6] In Ref. 7, the method was successfully used to simulate the steady, unsteady and aeroelastic cases for airfoils. In this paper, this method is extended to three-dimensional cases and used in the unsteady computation and flutter analysis of wings. During the unsteady computation process, the full boundary con-

*Post-Doctoral Researcher.

†Professor. Associate Fellow AIAA.

‡Researcher.

§Principal Research Scientist. Member AIAA.

¶Senior Research Engineer. Associate Fellow AIAA.

ditions for the Euler equations on the moving wings are replaced by approximate boundary conditions on the stationary grid around the undeformed wing surface at its mean position by using Taylor expansions. Since the deformation or displacement of the wing surface from its mean position is usually small in an aeroelastic problem, in particular, flutter simulations, we anticipate small errors by using such a simulation on a stationary grid, which can simply be the same grid used in the steady aerodynamic calculations.

The formulation of the proposed approximate boundary conditions is presented first. They are implemented in a three-dimensional body-fitted grid code, PARCAE(PARallel Computation of AeroElasticity)[8] developed at UCI. Numerical examples for unsteady and aeroelastic cases are given and results are compared with those obtained by the original PARCAE with full boundary conditions and the published experimental data.

II Governing Equations

The three-dimensional unsteady Euler equations in conservative integral form in the Cartesian coordinate system (x, y, z) are

$$\frac{\partial}{\partial t}\int_V \mathbf{W}dV + \int_S \mathbf{G}\cdot\mathbf{n}dS = 0 \tag{1}$$

where

$$\mathbf{W} = \begin{bmatrix} \rho \\ \rho u \\ \rho v \\ \rho w \\ \rho E \end{bmatrix} \tag{2}$$

$$\mathbf{G} = \begin{bmatrix} \rho(\mathbf{q}-\mathbf{q}_b) \\ \rho u(\mathbf{q}-\mathbf{q}_b) + p\mathbf{e}_x \\ \rho v(\mathbf{q}-\mathbf{q}_b) + p\mathbf{e}_y \\ \rho w(\mathbf{q}-\mathbf{q}_b) + p\mathbf{e}_z \\ \rho E(\mathbf{q}-\mathbf{q}_b) + p(u\mathbf{e}_x + v\mathbf{e}_y + w\mathbf{e}_z) \end{bmatrix} \tag{3}$$

$$\mathbf{q} = u\mathbf{e}_x + v\mathbf{e}_y + w\mathbf{e}_z \tag{4}$$

$$\mathbf{q}_b = u_b\mathbf{e}_x + v_b\mathbf{e}_y + w_b\mathbf{e}_z \tag{5}$$

$$E = \frac{1}{\gamma-1}\frac{p}{\rho} + \frac{1}{2}(u^2+v^2+w^2) \tag{6}$$

$$H = E + \frac{p}{\rho} \tag{7}$$

Following the procedure by Liu and Jameson,[9] a cell-centered finite volume method and Runge-Kutta multi-step scheme are used for the space discretization and time marching separately. Scalar and matrix artificial dissipation schemes are used to prevent oscillations near stagnation points and shock waves. In order to accelerate the computation, local time step and multi-grid are implemented. For unsteady cases, dual time-stepping is used to do the fully implicit time marching.[10]

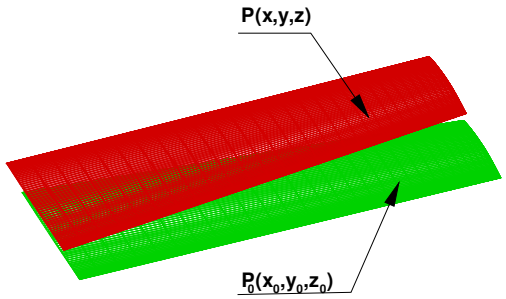

Fig. 1 Description of the movement of the wing.

III Simplified Boundary Conditions

For a wing with small deformation or movement, the original wing and the new position are considered as shown in Fig. 1. An arbitrary point $P_0(x_0,y_0,z_0)$ on the original wing moves to a new position P(x,y,z). For unsteady computation, the velocity boundary condition at P should be

$$\mathbf{q}\cdot\mathbf{n} = \mathbf{q}_b\cdot\mathbf{n} \tag{8}$$

where $\mathbf{q}_b$ is the velocity of the wing for unsteady cases and $\mathbf{n}$ is the unit normal vector at P. Using Taylor expansion, the flow variables at P can be represented by those at P_0:

$$\begin{aligned}\mathbf{q}(x,y,z) = \mathbf{q}(x_0,y_0,z_0) &+ \frac{\partial\mathbf{q}}{\partial x}(x_0,y_0,z_0)(x-x_0) \\ &+ \frac{\partial\mathbf{q}}{\partial y}(x_0,y_0,z_0)(y-y_0) \\ &+ \frac{\partial\mathbf{q}}{\partial z}(x_0,y_0,z_0)(z-z_0) + O(\Delta r^2)\end{aligned} \tag{9}$$

If the deformation of the wing surface is small, which means that $\Delta r = \sqrt{(x-x_0)^2+(y-y_0)^2+(z-z_0)^2} \ll 1$. For first-order approximation, we have

$$\mathbf{q}(x,y,z) = \mathbf{q}(x_0,y_0,z_0) + O(\Delta r) \tag{10}$$

Then equation (8) can be written as

$$\mathbf{q}(x_0, y_0, z_0) \cdot \mathbf{n} = \mathbf{q}_b \cdot \mathbf{n} \tag{11}$$

We can transform the above equation to a local grid coordinate system (ξ, η, ζ), and use the contravariant velocity (U, V, W). The relation between (U, V, W) and (u, v, w) is

$$\begin{aligned} u &= x_\xi U + x_\eta V + x_\zeta W \\ v &= y_\xi U + y_\eta V + y_\zeta W \\ w &= z_\xi U + z_\eta V + z_\zeta W \end{aligned} \tag{12}$$

Substituting equation (12) to equation (11), we get the following approximate wall boundary condition.

$$\begin{aligned} V = & \frac{(u_b n_x + v_b n_y + w_b n_z)}{(x_\eta n_x + y_\eta n_y + z_\zeta n_z)} \\ & - \frac{U(x_\xi n_x + y_\xi n_y + z_\xi n_z)}{(x_\eta n_x + y_\eta n_y + z_\zeta n_z)} \\ & - \frac{W(x_\zeta n_x + y_\zeta n_y + z_\zeta n_z)}{(x_\eta n_x + y_\eta n_y + z_\zeta n_z)} \end{aligned} \tag{13}$$

Notice in the above equation, although the flow velocities are evaluated at the stationary position P_0, the normal vector $\mathbf{n}$ is evaluated at the actual point P, which changes with time. In addition u_b,v_b and w_b, the local body velocity components, are also time dependent in an unsteady motion.

In the same way, we can deal with the normal momentum equation, which is used to compute the pressure on the wall.

$$\mathbf{n} \cdot [\frac{\partial \mathbf{q}}{\partial t} + (\mathbf{q} \cdot \nabla)\mathbf{q}] = \mathbf{n} \cdot (-\frac{\nabla p}{\rho}) \tag{14}$$

Since we are using first-order approximation in this paper, we use the first-order extrapolation to get the pressure on the wall from the first interior grid cells for both accurate and simplified boundary condition computations.

IV Results

A NACA0012 Unsteady Cases

Before we compute the aeroelastic cases, the pure unsteady cases are computed in this section. The simplified boundary condition method is implemented in a three dimensional code and used to calculate the flow over a NACA 0012 airfoil pitching around its quarter-chord point. Experimental data were provided by Landon.[11]

The instantaneous angle of attack of the airfoil is described by the following equation.

$$\alpha(t) = \alpha_m + \alpha_0 \sin \omega t \tag{15}$$

where ω and α_0 are the angular frequency and the amplitude of the pitching oscillation. The angular frequency ω is related to the reduced frequency defined as

$$\kappa = \frac{\omega c}{2U_\infty} \tag{16}$$

The AGARD CT case 5 of Ref. 11 is studied to validate the simplified boundary condition method. The airfoil is an NACA 0012 pitching at the free stream Mach number $M_\infty = 0.755, \alpha_m = 0.016°, \alpha_0 = 2.51°, \kappa = 0.0814$. The comparisons of the present inviscid computations with the experimental data of the instantaneous lift and moment coefficients vs. the instantaneous angle of attack are shown in Fig. 2. The lift coefficients predicted with the simplified boundary conditions are almost same as that predicted with accurate boundary condition method. They approach the experiment results at same level. But the moment coefficient result from the simplified boundary conditions is slightly worse than that with accurate boundary condition method. In order to find the reason why there are such differences for the coefficient, the first three Fourier components of the unsteady surface pressure distributions are shown in Fig. 3 and Fig. 4. Fig. 3 represents the real part of the pressure distribution and Fig. 4 represents the imaginary part. In those figures, the pressure from two different methods are almost same except the shock wave position. The shock wave predicted by the simplified-boundary-condition method is slightly downstream relative to that by the accurate boundary-condition method. This agrees with the findings for the two-dimensional cases in Ref. 7.

B AGARD 445.6 Wing

In this section, the simplified boundary condition is used to predict the flutter boundary for the three-dimensional AGARD 445.6 wing. The computational results are compared with the results from accurate boundary conditions and available experimental data.

The AGARD 445.6 wing is a semi-span model made of the NACA 65A004 airfoil that has a quarter-chord sweep angle of 45 degree, a panel aspect ratio of 1.65, and a taper ratio of 0.66. We consider the weakened wing model as listed in Ref. 12. It was tested in the Transonic Dynamic Tunnel at NASA Langley Center. Details of the wing could be found in Ref. 12. In order to compute the flutter boundary, different values of speed index V_f are tested. V_f is defined as

$$V_f = \frac{U_\infty}{b\omega\sqrt{\mu}} \tag{17}$$

Figures 5, 6, and 7 represent the comparison of the generalized displacements of the first mode between

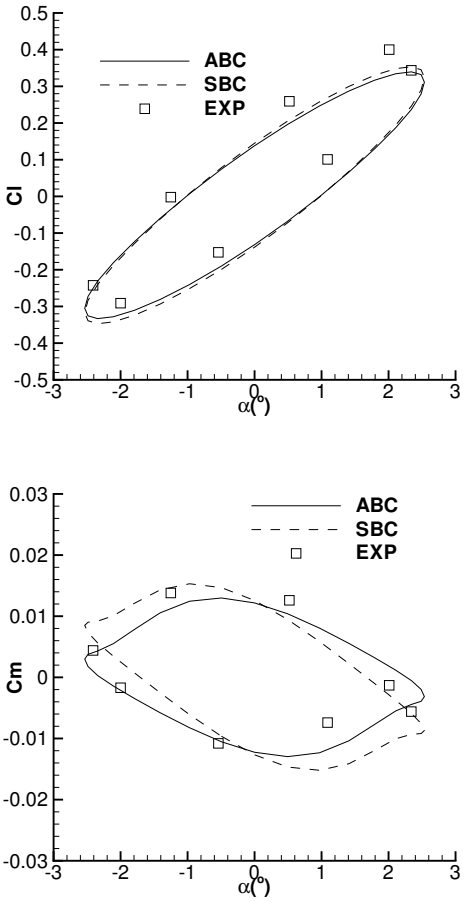

Fig. 2 Comparison of lift and moment coefficients between present computation and experiment, NACA 0012, $M_\infty = 0.755$, $\alpha_m = 0.016°$, $\alpha_0 = 2.51°$, $\kappa = 0.0814$.

the solution with the accurate boundary conditions and that with simplified boundary conditions at Mach number 0.96 stable, the neutrally stable, and unstable case respectively. In these figures, the results from the simplified-boundary-condition method coincide with those with the accurate boundary-condition method.

Finally, the comparison of the flutter boundary is shown in Fig. 8. The computation result predicted by the simplified boundary conditions is compared with computation result by the accurate-boundary-condition method and the experiment result.[13] Both the simplified-boundary-condition method and the accurate-boundary-condition method predict the transonic dip and their results approach the experimental results in subsonic and transonic Mach number range. They departure from the experiment results in supersonic range.

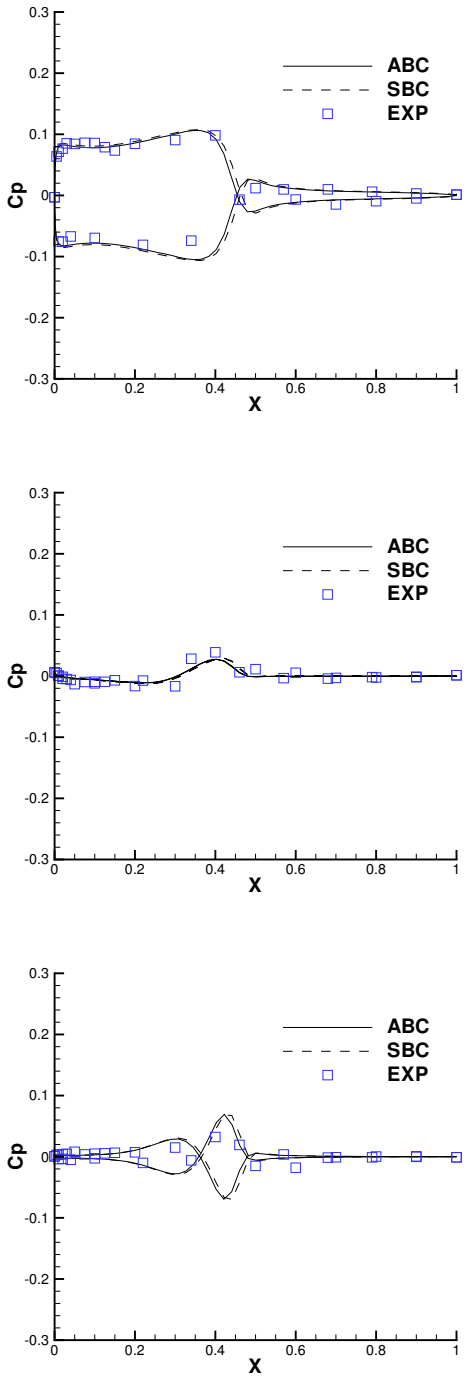

Fig. 3 Comparison of computational surface pressure distribution of NACA 0012 with experimental data, $M_\infty = 0.755$, $\alpha_m = 0.016°$, $\alpha_0 = 2.51°$, $\kappa = 0.0814$ **(Real part) .**

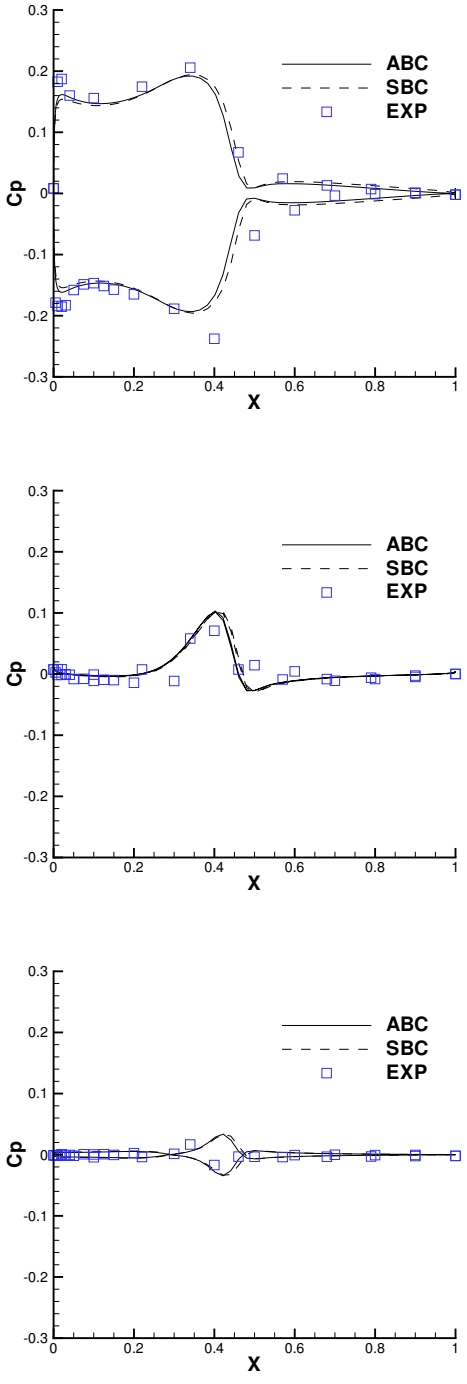

Fig. 4 Comparison of computational surface pressure distribution of NACA0012 with experimental data, $M_\infty = 0.755$, $\alpha_m = 0.016°$, $\alpha_0 = 2.51°$, $\kappa = 0.0814$ (Imaginary part).

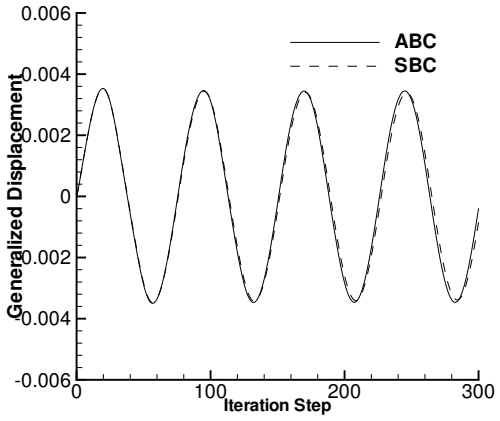

Fig. 5 Time history of the generalized displacement of the first mode for AGARD 445.6 wing model for M_∞=0.960, V_f =0.25(Stable case).

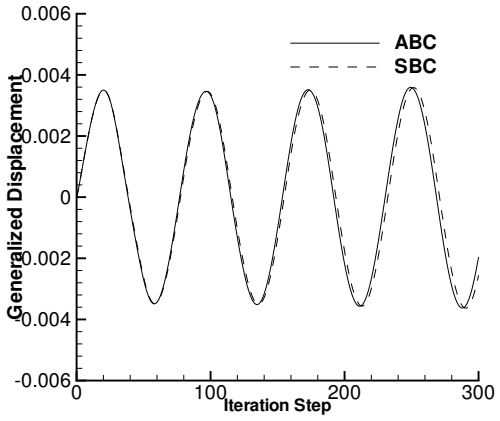

Fig. 6 Time history of the generalized displacement of the first mode for AGARD 445.6 wing model for M_∞=0.960, V_f =0.26(Neutral case).

V Summary and Conclusion

A small-perturbation-boundary-condition method is extended to three dimensions and used for airfoil and wing unsteady/flutter computations. The CFD solver with the small-perturbation-boundary-condition is coupled with the elastic equations to predict the aeroelastic properties of the AGARD wing. During the unsteady/aeroelastic computation process, the accurate nonlinear Euler equations are solved in the flow field, while the movement and deformation of the solid wall is accounted for in the new approximate boundary conditions without moving or deforming the computational grids. The first-order simplified boundary conditions are used in solving the full Euler equations for unsteady two dimensional and three dimen-

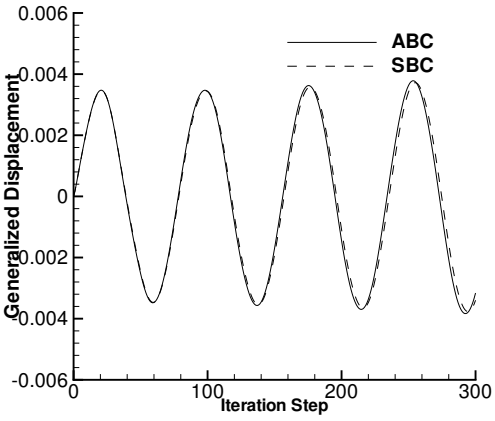

Fig. 7 Time history of the generalized displacement of the first mode for AGARD 445.6 wing model for M_∞=0.960, V_f =0.27(Unstable case).

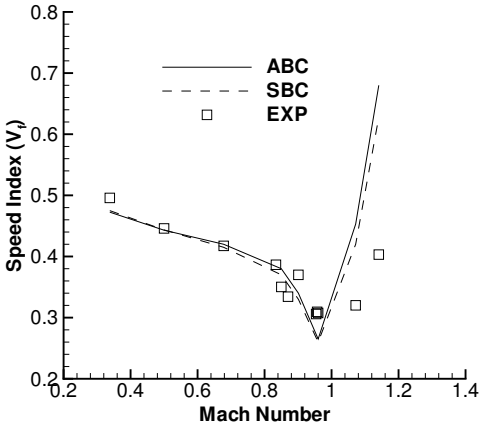

Fig. 8 Comparison the flutter boundary of AGARD 445.6 Wing.

sional aeroelastic cases. The results are compared with Euler solutions with the full boundary conditions on moving grids and known experimental data. The comparison shows that the simplified-boundary-condition method is accurate enough for unsteady cases and flutter cases where the perturbations are small.

References

[1]Schuster, D. M., Liu, D. D., and Huttsell, L. J., "Computational Aeroelasticity: Success, Progress, Challenge," *Journal of Aircraft*, Vol. 40, No. 5, Sep.-Oct. 2003, pp. 843–856.

[2]Batina, J. T., "A Finite-Difference Approximate-Factorization Algorithm for Solution of the Unsteady Transonic Small-Disturbance Equation," NASA TP 3129, Jan. 1992.

[3]Edwards, J., "Transonic Shock Oscillations Calculated with a New Interactive Boundary Layer Coupling Method," AIAA Paper 93-0777, 1993.

[4]Edwards, J., "Transonic Shock Oscillations and Wing Flutter Calculated with an Interactive Boundary Layer Coupling Method," *EUROMECH-Colloquium 349, Simulation of Fluid-Structure Interaction in Aeronautics*, Gottingen, Germany, Sept. 1996.

[5]Gao, C., Luo, S., Liu, F., and Schuster, D. M., "Calculation of Unsteady Transonic Flow by an Euler Method with Small Perturbation Boundary Conditions," AIAA Paper 2003-1267, Jan. 2003.

[6]Gao, C., Luo, S., Liu, F., and Schuster, D. M., "Calculation of Airfoil Flutter by an Euler Method with Approximate Boundary Conditions," AIAA Paper 2003-3830, June 2003.

[7]Yang, S., Luo, S., Liu, F., Cai, H.-M., and Shuster, D. M., "Time-Domain Aeroelastic Simulation on Stationary Body-Conforming Grids with Small Perturbation Boundary Conditions," AIAA Paper 2004-0885, Jan. 2004.

[8]Sadeghi, M., Yang, S., and Liu, F., "Parallel Computation of Wing Flutter with a Coupled Navier-Stokes/CSD Method," AIAA Paper 2003-1347, Jan. 2003.

[9]Liu, F. and Jameson, A., "Multigrid Navier-Stokes Calculations for Three-Dimensional Cascades," *AIAA Journal*, Vol. 31, No. 10, October 1993, pp. 1785–1791.

[10]Liu, F. and Ji, S., "Unsteady flow calculations with a multigrid Navier-Stokes method," *AIAA Paper 95-2205*, June 1995.

[11]Landon, R. H., "NACA 0012 Oscillating and Transient Pitching, Compendium of Unsteady Aerodynamic Measurements, Data Set 3," AGARD Report R-702, Aug. 1982.

[12]Yates Jr., E. C., Land, N. S., and Foughner, J. T., "Measured and Calculated Subsonic and Transonic Flutter Characteristics of a 45° Swepteback Wing Planform in Air and in Freon-12 in the Langley Transonic Dynamics Tunnel," NASA TN D-1616, March 1963.

[13]Yates Jr., E. C., "AGARD Standard Aeroelastic Configurations for Dynamic Response, I – Wing 445.6," NASA TM 100492, Aug. 1987.